Resource

Cell

Exploring the Mode-of-Action of Bioactive Compounds by Chemical-Genetic Profiling in Yeast

Ainslie B. Parsons,[1,2,11] Andres Lopez,[1,11] Inmar E. Givoni,[3,4,11] David E. Williams,[5] Christopher A. Gray,[5] Justin Porter,[5] Gordon Chua,[1] Richelle Sopko,[1,2] Renee L. Brost,[1] Cheuk-Hei Ho,[1,2] Jiyi Wang,[6] Troy Ketela,[7] Charles Brenner,[8] Julie A. Brill,[2] G. Esteban Fernandez,[9] Todd C. Lorenz,[9] Gregory S. Payne,[9] Satoru Ishihara,[10] Yoshikazu Ohya,[10] Brenda Andrews,[1,2] Timothy R. Hughes,[1,2] Brendan J. Frey,[1,3,4] Todd R. Graham,[6] Raymond J. Andersen,[5] and Charles Boone[1,2,*]

[1] Banting and Best Department of Medical Research, University of Toronto, Toronto, Ontario M5G 1L6, Canada
[2] Department of Molecular and Medical Genetics, University of Toronto, Toronto, Ontario M5S 1A8, Canada
[3] Probabilistic and Statistical Inference Group, Departments of Electrical and Computer Engineering and Computer Science, University of Toronto, Toronto, Ontario M5S 3G4, Canada
[4] Department of Electrical and Computer Engineering, University of Toronto, Toronto, Ontario M5S 3G4, Canada
[5] Department of Chemistry, Earth & Ocean Sciences, University of British Columbia, Vancouver, British Columbia V6T 1Z1, Canada
[6] Department of Biological Sciences, Vanderbilt University, Nashville, TN 37235, USA
[7] Infinity Pharmaceuticals, Inc., Cambridge, MA 02130, USA
[8] Department of Genetics, Dartmouth Medical School, Lebanon, NH 03756, USA
[9] Department of Biological Chemistry, David Geffen School of Medicine UCLA, Los Angeles, CA 90095, USA
[10] Department of Integrated Biosciences, Graduate School of Frontier Sciences, University of Tokyo, Kashiwa, Chiba Prefecture 277-8562 Japan
[11] These authors contributed equally to this work.
*Contact: charlie.boone@utoronto.ca
DOI 10.1016/j.cell.2006.06.040

SUMMARY

Discovering target and off-target effects of specific compounds is critical to drug discovery and development. We generated a compendium of "chemical-genetic interaction" profiles by testing the collection of viable yeast haploid deletion mutants for hypersensitivity to 82 compounds and natural product extracts. To cluster compounds with a similar mode-of-action and to reveal insights into the cellular pathways and proteins affected, we applied both a hierarchical clustering and a factorgram method, which allows a gene or compound to be associated with more than one group. In particular, tamoxifen, a breast cancer therapeutic, was found to disrupt calcium homeostasis and phosphatidylserine (PS) was recognized as a target for papuamide B, a cytotoxic lipopeptide with anti-HIV activity. Further, the profile of crude extracts resembled that of its constituent purified natural product, enabling detailed classification of extract activity prior to purification. This compendium should serve as a valuable key for interpreting cellular effects of novel compounds with similar activities.

INTRODUCTION

Determining the mode-of-action of new compounds is a central problem in chemical biology. Rich functional information can be obtained from scoring ~5000 viable yeast haploid deletion mutant strains for hypersensitivity to a diverse set of compounds, a process termed chemical-genetic profiling (Parsons et al., 2004). Gene deletions that render cells hypersensitive to a specific drug identify pathways that buffer the cell against the toxic effects of the drug and thereby provide clues about its mode-of-action (Giaever et al., 2004; Lum et al., 2004; Parsons et al., 2004). As outlined conceptually for drug-induced changes in global patterns of gene expression (Hughes et al., 2000; Marton et al., 1998), an emerging view is that compounds with similar biological effects lead to similar chemical-genetic profiles (Brown et al., 2006; Lee et al., 2005). Thus, a compendium of chemical-genetic profiles should provide a data set that will both allow for organization of both compounds and yeast genes into functionally relevant groups and also identify sets of compounds with similar biological effects and genes whose deletion leads to sensitivity to similar compound sets. Ultimately, the integration of large-scale genetic interaction data obtained from genome-wide synthetic lethal screens (Tong et al., 2001, 2004) and chemical-genetic data should provide a system for linking compounds to their target pathway (Parsons et al., 2004).

Many compounds are in limited supply, and thus a major challenge is to screen the collection of yeast deletion mutants efficiently. Parallel fitness tests of large numbers of pooled deletion strains in a minimal amount of medium is possible due to the unique molecular barcodes that tag and identify each deletion strain (Giaever et al., 2002; Shoemaker et al., 1996). Here, we tested 82 chemical perturbations against the yeast haploid deletion collection using parallel fitness tests. Hierarchical clustering analysis and probabilistic sparse matrix factorization of the compendium of chemical-genetic interaction profiles reveals numerous insights into the pathways and proteins affected by drug treatments. In particular, we show that tamoxifen, a breast cancer therapeutic, disrupts calcium homeostasis, and we identify PS as a target for papuamide B, a cytotoxic cyclic lipopeptide with antifungal and anti-HIV activity (Ford et al., 1999).

RESULTS

A Compendium of Chemical-Genetic Profiles

We generated chemical-genetic profiles for 82 different conditions by screening them against the yeast haploid deletion collection. Included in this group are 75 synthetic compounds and natural products, of which 23 are FDA approved, and 7 crude antifungal extracts, derived from different marine sponges and microorganisms. The list of chemicals, the experimental concentrations, and a brief comment on their mode-of-action are included in Table 1. To mine information from our compendium we applied two data visualization and analysis techniques to the dataset: two-dimensional hierarchical clustering and probabilistic sparse matrix factorization (PSMF) analysis.

Two-Dimensional Hierarchical Clustering Analysis

The set of chemical-genetic profiles was visualized by two-dimensional hierarchical clustering (Figure 1). This data matrix contains all chemical-genetic interactions where the combined average $\log_2$ ratio (control/experiment) of both barcodes (uptag and downtag) corresponding to each strain is greater than 0.5, meaning that the drug treatment leads to at least a 1.4-fold depletion of the deletion mutant relative to the control. Prior to clustering, we processed the data by removing a set of 121 genes whose corresponding deletion mutant displayed statistically significant multidrug sensitivity (Table S2). This multidrug-resistant gene set includes genes whose deletion leads to increased membrane permeability, including *ERG2*, *ERG5*, and *ERG6,* as well as *PDR5,* which encodes a drug-efflux pump, and *PDR1*, encoding a transcription factor that regulates genes involved in multidrug resistance. In total, 82 conditions were clustered on the vertical axis, based upon the overlap of their chemical-genetic profiles, and 3418 genes were clustered on the horizontal axis, according to their overlapping patterns of compound sensitivities.

Clustering Chemical-Genetic Profiles for Compounds with Similar Modes-of-Action and Genes with Similar Function

We found that compounds with similar cellular effects showed similar chemical-genetic profiles and thereby cluster together on the vertical axis in Figure 1, revealing both anticipated and novel insights into their mode-of-action. In particular, there are a number of examples where the cluster analysis groups compounds known to inhibit the same pathway or target (Figure 1, individual clusters indicated by roman numerals): (i) actin binding agents latrunculin B (Ayscough et al., 1997) and cytochalasin A (Torralba et al., 1998); (ii) cell wall synthesis inhibitors staurosporine, which targets Protein kinase C, a regulator of a MAP kinase cascade involved in cell wall metabolism (Yoshida et al., 1992), and caspofungin, which inhibits 1,3 β-glucan synthase (Douglas et al., 1994b); (iii) nystatin (Hosono, 2000) and amphotericin (Aoun, 2000), both of which act by increasing the permeability of the fungal cell membrane; (iv) clotrimazole and fluconazole, chemical analogs and antifungal agents that target Erg11 (Fromtling, 1988; Truan et al., 1994), a protein encoded by an essential gene in the ergosterol biosynthesis pathway; (v) radicicol and geldanamycin, although structurally unrelated, both act as highly selective inhibitors of Hsp90 function through their ability to bind within the ADP/ATP binding pocket of the chaperone (Roe et al., 1999); (vi) benomyl (Thomas et al., 1985) and nocodazole (Kunkel, 1980), two microtubule poisons; (vii) haloperidol (Moebius et al., 1996), fenipropimorph (Marcireau et al., 1990), and dyclonine (Hughes et al., 2000), are all thought to inhibit Erg2 function in yeast. Deletion mutants with similar chemical sensitivities also cluster together on the horizontal axis of Figure 1, grouping functionally related genes (Figure S1).

Probabilistic Sparse Matrix Factorization Analysis

Two-dimensional hierarchical clustering is limited by its inability to associate a gene or compound with more than one group. In order to discover links between compound activities that may not be revealed by hierarchical clustering, we used probabilistic sparse matrix factorization (PSMF) (Dueck et al., 2005). In hierarchical clustering, each mutant has a chemical sensitivity signature in response to a set of compounds, and mutants are linked together based on a comparison of all compounds. In a factorization analysis, chemical sensitivity signatures are linked together based on a variety of subsets of compounds. This allows the same mutant to be linked to multiple other mutants based on different subsets of compounds. Each compound in the subset can have a different importance and different subsets can overlap. We refer to each subset of compounds detected by the algorithm as a factor. Each mutant's sensitivity signature can be represented as a weighted sum of factors.

Techniques other than PSMF can be used to factorize matrix data; however, PSMF has been previously applied to microarray data, where it was shown to achieve a higher rate of significant clusters/factors discovery compared to

Table 1. Chemicals and Natural Product Extracts Screened in This Study

Compound	Inhibitory Concentration	Comments
(−)-Abietic acid	0.33 mM	major component of oleoresin synthesized by conifer species, inhibits lipoxygenase activity
(+/−) Coniine	5% (v/v)	poisonous teratogenic piperidine alkaloid
(+)-Usnic acid	61 μM	dibenzofuran derivative, various biological activities (i.e., antibiotic, anti-inflammatory)
(1*R*, 2*S*, 5*R*) - (−) - Menthol	480 μM	terpene alcohol used as a flavoring
(*S*)-(+)-Camptothecin	30 μM	topoisomerase I inhibitor
1-10 Phenanthroline monohydrate	0.02 μM	metal chelator that inhibits Pol II by sequestering magnesium
2-Hydroxyethilhidrazine	5% (v/v)	inhibits the phospholipid methylation in yeast
4-Hydroxytamoxifen	36.1 μM	metabolite of tamoxifen
Actinomycin D	37 μM	binds to DNA and inhibits RNA synthesis
Agelasine E	0.03 μM	unknown target
Alamethicin[a]	59.3 μM	cyclic nonadecapeptide antibiotic that can act as an ionophore
Amantadine hydrochloride	5.9 mM	polycyclic cage compound with antiviral and anti-Parkinsonian activities
Amiodarone hydrochloride	150 μM	antianginal and antiarrhythmic drug
Amphotericin B	0.76 μM	compromises cell membrane integrity
Anisomycin	3.8 μM	protein synthesis inhibitor, inhibits peptidyl transferase in eukaryote ribosomes
Artemisinin	88.5 μM	antimalarial sesquiterpene lactone, inhibits the SERCA ortholog of *Plasmodium falciparum*
Basiliskamide	0.26 μM	unknown target
Benomyl	0.12 μM	Microtubule-depolymerizing agent
Brefeldin A	0.36 μM	secretory pathway inhibitor
Caffeine	3.1 mM	phosphodiesterase inhibitor
Calcium ionophore A23187	191 μM	calcium ionophore
Caspofungin	7 nM	inhibits synthesis of glucan, a component of the yeast cell wall
Cerulenin	1.6 μM	inhibits the elongation of fatty acids
Chlorpromazine hydrochloride	28.2 μM	prototypical phenothiazine antipsychotic drug
Cisplatin	0.17 mM	DNA inter- and intracross linking agent
Clomiphene citrate	4.9 μM	stilbene derivative structurally related to chlorotrianisene
Clotrimazole	0.4 nM	inhibitor of ergosterol biosynthesis in yeast
Cyclopiazonic acid	0.4 mM	sarcoplasmic reticulum Ca^{2+}- ATPase inhibitor
Cytochalasin A	21 μM	inhibits actin polymerization
Desipramine hydrochloride	231 μM	used to treat depression and other mood disorders
Doxycycline hyclate	1.12 mM	antibiotic
Dyclonine hydrochloride	55.2 μM	local anaesthesic, inhibits the ergosterol pathway
Emetine dihydrochloride hydrate	1.25 mM	protein synthesis inhibitor
Emodin	0.4 mM	casein kinase II inhibitor
Extract 00-132	32 μg/ml	antifungal natural product extract
Extract 00-192	15 μg/ml	antifungal natural product extract
Extract 00-243	10 μg/ml	antifungal natural product extract

(*Continued on next page*)

Table 1. ***Continued***

Compound	Inhibitory Concentration	Comments
Extract 00-303C	29 μg/ml	antifungal natural product extract
Extract 00-89	5 μg/ml	antifungal natural product extract
Extract 6592	130 μg/ml	antifungal natural product extract
Extract 95-57	30 μg/ml	antifungal natural product extract
Fenpropimorph	0.00001%(v/v)	morpholine fungicide used in agriculture, inhibits sterol isomerase and sterol reductase
FK506	9 nM	immunosuppressant drug, inhibits calcinuerin function in yeast
Fluconazole	0.03 μM	inhibitor of ergosterol biosynthesis in yeast
Geldanamycin	36 nM	HSP90 inhibitor
Haloperidol	0.1 mM	a butyrophenone antipsychotic drug used to treat schizophrenia, binds the sigma receptor
Harmine hydrochloride	241.2 μM	β-carboline alkaloid, cytotoxic activities against human tumor cell lines
Hoechst 33258	93.7 μM	DNA minor groove binding agent
Hydrogen peroxide	0.4%(v/v)	oxidizing agent
Hydroxyurea	20 mM	DNA-damaging agent, inhibits ribonuclease reductase
Hygromycin B	8 nM	aminoglycoside antibiotic
Latrunculin B	30 μM	actin-depolymerizing agent
LY 294002 hydrochloride	290 μM	mammalian PI3 kinase inhibitor
Methanesulfonic acid methyl ester (MMS)	0.004%	DNA-alkylating agent
Mitomycin C	0.15 μM	DNA-damaging agent
Neomycin B trisulfate salt hydrate	150 μM	aminoglycoside antibiotic, inhibits ribozyme function
Nigericin	69 μM	polyether antibiotic and ionophore
Nocodazole	10 μM	Microtubule-depolymerizing agent
Nystatin dihydrate	0.7 μM	compromises cell membrane integrity
Oligomycin[b]	127 μM	inhibits membrane bound mitochondrial ATPase
Papuamide B	0.4 μM	natural product of unknown target
Parthenolide	141 μM	sesquiterpene lactone with anti-inflammatory properties
Pentamidine isethionate	130 μM	antiprotozoal agent
Phenylarsine oxide	8 μM	phosphatidylinositol 4-kinase inhibitor
Plumbagin	4.2 μM	naphtaquinone derivative that induces cell death through generation of reactive oxygen species
Radicicol	49.3 μM	macrolactone protein tyrosine kinase inhbitor; HSP90 inhibitor
Raloxifene hydrochloride	1.05 mM	estrogen antagonist
Rapamycin	5.5 pM	inhibitor of TOR kinase signaling
Sodium azide	77 μM	cytochrome oxidase inhibitor
Staurosporine	3 μM	PKC inhibitor
Stichloroside	1 nM	unknown target, active compound from extract 00-192
Sulfometuron methyl	0.2 nM	inhibitor of amino acid biosynthesis
Tamoxifen	5.4 μM	competitively inhibits estradiol binding to estrogen receptor
Theopalauamide	0.4 nM	unknown target, active compound from extract 00-132
Thialysine	3 μM	toxic lysine analog

Table 1. *Continued*

Compound	Inhibitory Concentration	Comments
Trichostatin A	99.2 μM	histone deacetylase inhibitor
Trifluoroperazine dihydrochloride	11 μM	phenothiazine with actions similar to chlorpromazine
Tunicamycin	71 pM	inhibitor of protein glycosylation
U-73122	0.2 μM	phospholiapse C inhibitor
Valinomycin	2.2 μM	potassium selective ionophore
Verrucarin	2 μM	macrocyclic trichothecene; protein synthesis inhibitor
Wortmannin	0.3 nM	inhibitor of phosphatidylinositol kinase signalling

NA: Not applicable.
Inhibitory concentration refers to the screening concentration. Complete table including CAS numbers, FDA status, source, site of collection, and references in Table S1.
[a]A mixture of alamethicin analogs.
[b]A mixture of oligomycins A, B, and C.

hierarchical clustering or other factorization techniques, including principal and independent components analysis (Dueck et al., 2005). A particular advantage of PSMF over another multiway factorizating technique, bi-clustering (Cheng and Church, 2000), is that PSMF allows each cluster to be defined by an arbitrary set of genes and compounds, whereas bi-clustering is restricted so that any two clusters containing the same gene (or compound) must be defined by exactly the same set of genes (or compounds). In related work, variational inference in a labeled latent Dirichlet allocation process was used to analyze chemical-genetic profiles (Flaherty et al., 2005), but this analysis employed prior knowledge of gene functions (MIPS annotations), whereas our PSMF analysis altogether avoids the need for gene function annotations.

In this analysis, we identified 30 factors and represented each signature as a weighted sum of up to three factors. By detecting a factor, the algorithm is identifying compounds that have a similar effect on a specific group of mutants. The factors can correlate to different cellular functions; for example, compounds that inhibit DNA synthesis and repair may form one factor because a group of mutants sensitive to those compounds display similar sensitivity. Thus, the factorization approach gives a complete representation of groups of related compounds that affect groups of related mutants, while allowing for each mutant and each compound to be linked to more than one cellular function.

The "factorgram" (Cheung et al., 2006) shown in Figure 2 is a visualization of the factorization results as applied to the compendium of chemical-genetic profiles. Each factor is visually represented by a block of data showing the original data matrix entries for the subset of the compounds in that factor, and the subset of mutants which are most significantly affected by the given factor. The factors are shown along the diagonal of Figure 2.

Four detailed examples of factors and the subsets of strains utilizing specific factors are shown in Figures 2A–2D. The group of compounds present in the factor is listed along the *x* axis, with the most important compound on the left. Along the *y* axis are strains using that factor, with the most significant strain at the top. For example, in Figure 2A, papuamide B and alamethicin are the compounds that are most important in factor number 5, and this is driven by the common sensitivity of the deletion mutants listed on the *y* axis, with the most significant mutants at the top (*hoc1Δ*, *pps1Δ*, *ypl158cΔ,* and so on).

One group that emerged from the PSMF analysis is that of the DNA-damaging agents, linking together in factor 21, as expected, the similar activities of mitomycin C, MMS, camptothecin, cisplatin, and hydroxyurea (Figure 2B). However, an additional component of that factor is actinomycin, an antibiotic that binds to DNA and inhibits RNA synthesis (Sobell, 1985). Interestingly, this compound does not cluster next to the DNA-damage agents in Figure 1 but instead clusters virtually on its own. The mutants defined by this profile (including*TOP3*, *MUS81*, and *RAD52;* i.e., the deletion mutants which are hypersensitive to camptothecin) are enriched for lesions in DNA replication and repair.

In a second example, verrucarin and neomycin sulfate are two compounds linked by PSMF analysis (factor 6; Figure 2C) and not by hierarchical clustering. Verrucarin inhibits protein synthesis in yeast (Hernandez and Cannon, 1982) and neomycin sulfate is an aminoglycoside antibiotic that inhibits protein translation (Schroeder et al., 2000). The deletion mutants utilizing that factor include many cytoplasmic ribosomal small subunit deletion mutants and translation initiation factors, in accordance to the mode-of-action of the compounds.

Chemical-Genetic Profiling of Crude Extracts Containing Bioactive Natural Products

Because chemical-genetic profiling is applicable to any compound that impairs yeast cell growth, it can also be applied to natural product extracts, which appear to often contain only one growth-inhibitory compound. To test whether chemical-genetic profiling may be particularly useful for classifying natural product extracts prior to

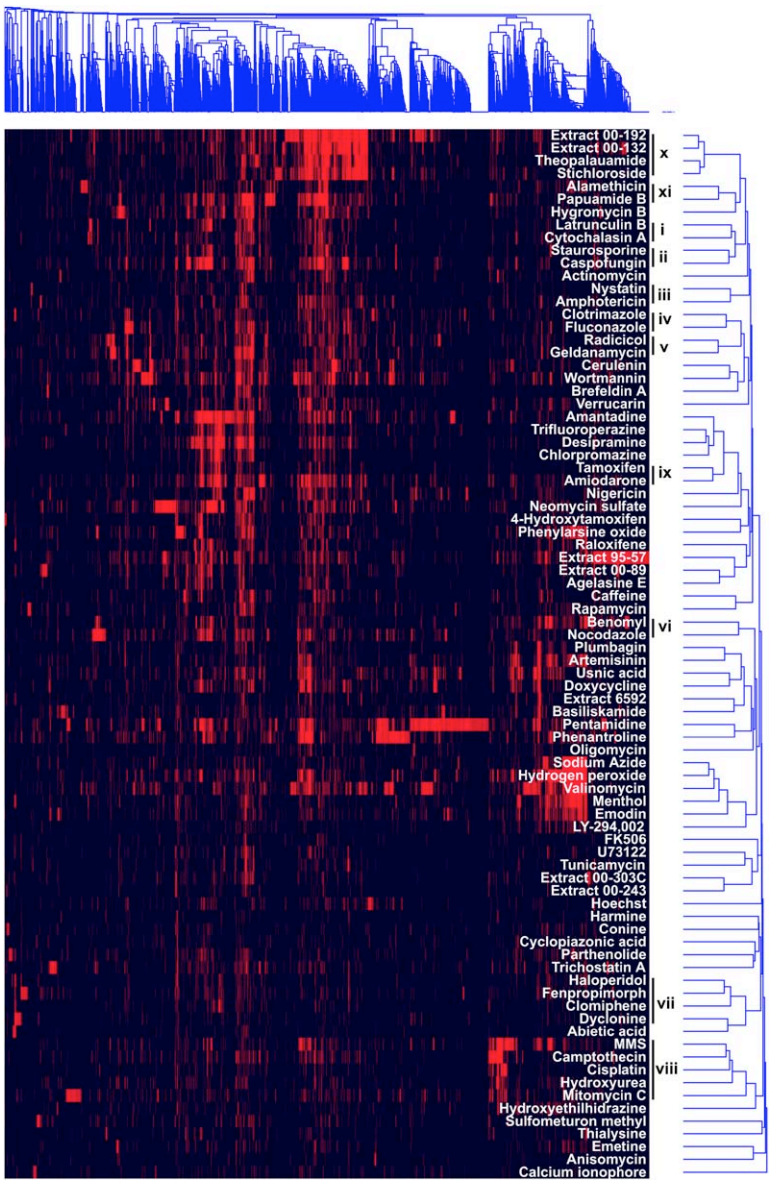

Figure 1. Two-Dimensional Hierarchical Clustering Analysis of Chemical-Genetic Profiles

Eighty-two conditions, including 75 compounds and 7 crude extracts, were clustered. 3418 genes are plotted on the horizontal axis with the gene cluster tree above. Compounds are plotted on the vertical axis with the cluster tree on the outermost right side of the plot. Chemical-genetic interactions are represented as red lines. Compound clusters are labeled with roman numerals as referenced in the text.

embarking on the time-consuming purification of the active component, we examined the profiles of 7 different antifungal extracts derived from marine sponges and microorganisms. Surprisingly, two of the extracts derived from different organisms and diverse locations, extract 00-192, from a sea cucumber from the Commonwealth of Dominica and extract 00-132, derived from an Indonesian marine sponge, showed highly similar chemical-genetic profiles, resembling the reproducibility we observe for repeated screens of the same compound (Figure 3A). Moreover, they clustered together within the compendium (Figure 1, cluster x) and were linked by PMSF analysis (factor 29; Figure 2D). Thus, the two extracts appear to contain antifungal compounds with similar modes of action.

We purified antifungal compounds from the two crude extracts. The compound isolated from extract 00-192 was identical to stichloroside (Kitagawa et al., 1981), whereas the compound isolated from extract 00-132 was identical to theopalauamide (Schmidt et al., 1998). Both of the purified compounds display chemical-genetic profiles resembling those of their crude extracts (Figure 1, cluster x), confirming that these compounds are responsible for the antifungal activity within the extracts. The two compounds do not share structural features and thus chemical-genetic profiling appears to have linked molecules with disparate chemistry to the same biological activity (Figure 3B).

Drug-resistant mutants often result from mutations in the target gene or pathway (Douglas et al., 1994b; Fried and Warner, 1982; Heitman et al., 1991). To obtain further evidence for a similar mode-of-action between the two compounds, we isolated stichloroside-resistant mutants

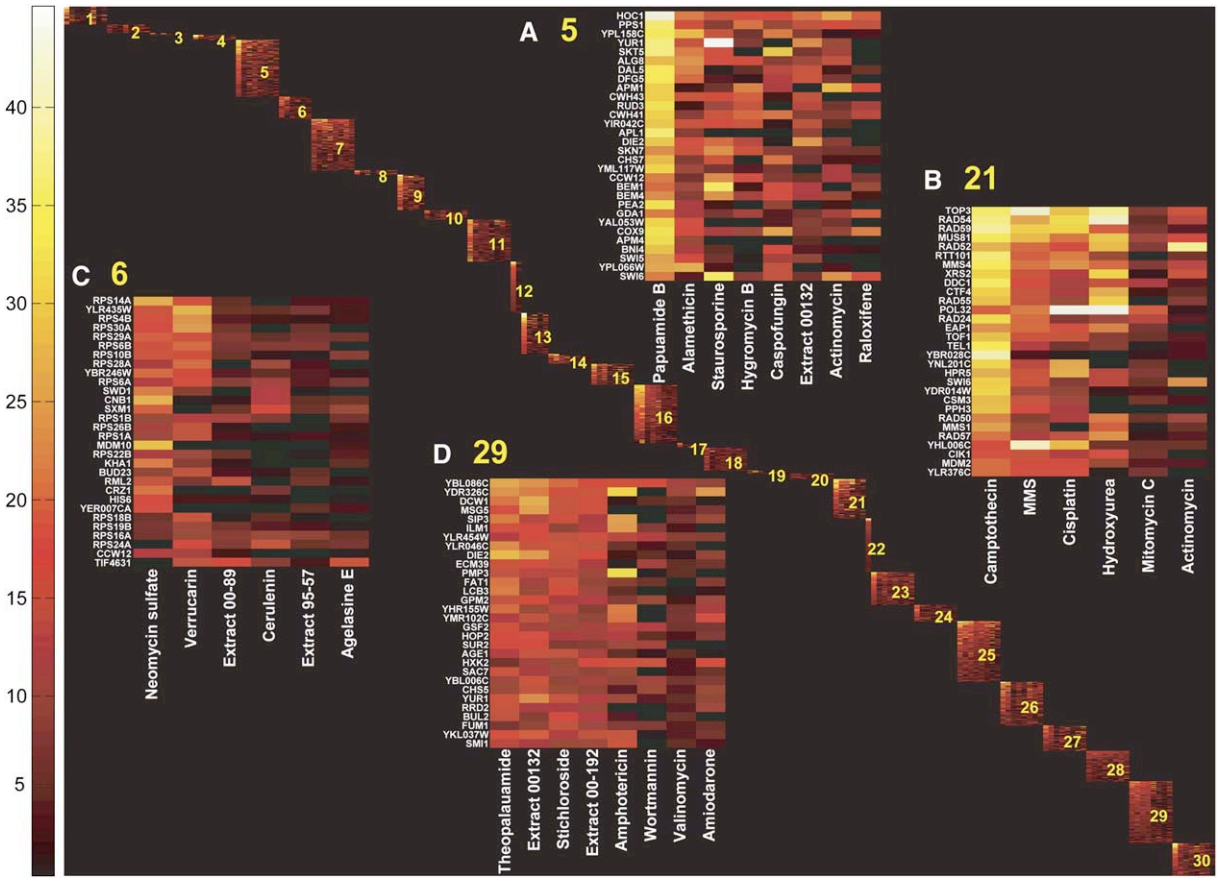

Figure 2. Visualization of Results from PSMF

Each numbered block along the diagonal shows the data that contributed to a particular factor and displays the mutants and compounds discovered by PSMF. The statistically significant mutants utilizing each factor are shown along the vertical axis and are sorted according to the weighting of the factor in explaining the chemical-sensitivity profile for the mutant. The subset of compounds significantly present in each factor are shown along the horizontal axis and are sorted according to their importance within the factor. Compounds and strains may appear several times. Color bar on the left indicates the scale of the normalized data (see Experimental Procedures). An expanded view of several blocks are detailed: (A) factor number 5, (B) factor 21, (C) factor 6, (D) factor 29. Each expanded view shows the 8 most important compounds and the 30 most significant mutants.

and then tested the mutants for theopalauamide resistance. Four independent strains were isolated as resistant to extract 00-192 and were subsequently confirmed to be resistant to its active compound, stichloroside. For each of the four strains, the resistance was attributable to a single recessive mutation, and the mutants fell into two complementation groups (00-192-RA and 00-192-RB). If stichloroside and theopalauamide function similarly, the stichloroside-resistant mutants should also display theopalauamide resistance, and indeed we found this to be true (Figure 3C). The identities of the genes affected by the mutations conferring the drug resistance are not known, but neither is linked to *PDR1* or *PDR3*, two genes involved in general multidrug resistance. In addition, the resistant phenotype is specific because the mutants displayed wild-type sensitivity to cycloheximide, caspofungin, and papuamide B (data not shown). We conclude that stichloroside and theopalauamide share a common mode-of-action in yeast and that chemical-genetic profiling is an effective means for functional classification of natural product extracts.

Compendium Reveals Insights into the Activities of Human Therapeutics

Interestingly, the chemical-genetic interaction profile of amiodarone, an antianginal and antiarrhythmic drug, clusters with tamoxifen, a competitive inhibitor of estradiol binding to the estrogen receptor and a common breast cancer drug (Figure 1, cluster ix). The antifungal activity of amiodarone appears to be related to its mode-of-action in human cells and is associated with the perturbation of calcium homeostasis, resulting in an increase in cytosolic Ca^{2+} to toxic levels through an influx of external Ca^{2+} and release of internal Ca^{2+} stores into the cytosol upon drug exposure (Courchesne, 2002; Courchesne and Ozturk, 2003; Gupta et al., 2003). The resemblance of the chemical-genetic profiles of amiodarone and tamoxifen indicates that the physiological effects of these drugs on

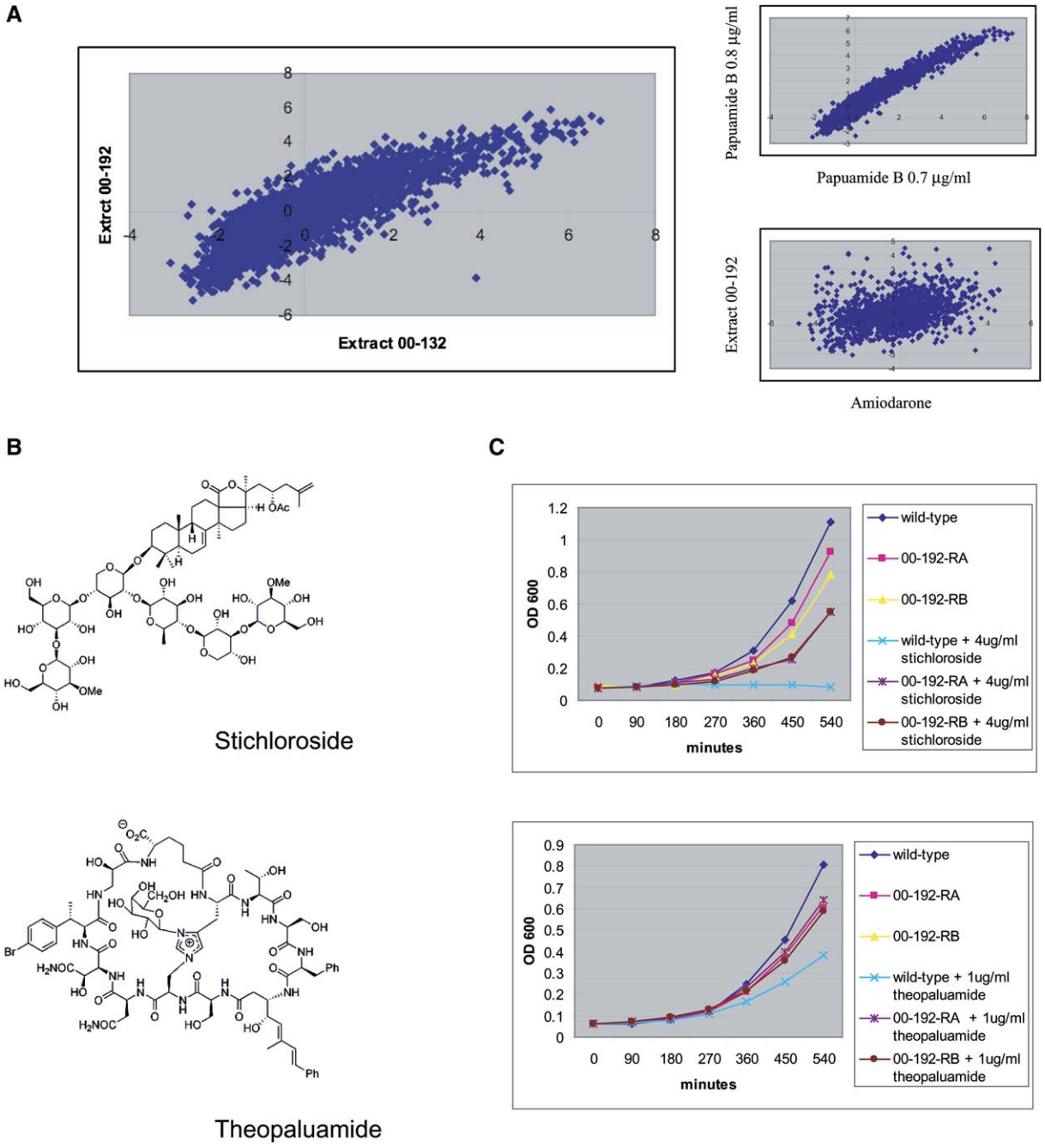

Figure 3. Chemical-Genetic Analysis of Natural Product Extracts

(A) Correlation plot between chemical-genetic screens of extract 00-132, derived from a marine sponge collected in Indonesia, and extract 00-192, derived from a sea cucumber collected in the Dominican Republic (correlation coefficient (r) = 0.892). Points on the plot correspond to the $\log_2$ ratio of control signal/drug-treated signal for each barcode in the two screens. For comparison purposes, a correlation plot showing two pap B screens at similar concentrations (0.8 and 0.7 µg/ml; r = 0.953) is shown as well as a plot depicting two different chemical treatments (extract 00-192 and amiodarone; r = 0.533).

(B) Structures of stichloroside and theopalauamide. Stichloroside is the active compound derived from crude extract 00-192 and theopaluamide is the active compound present in crude extract 00-132.

(C) Cross-resistance of extract 00-192 resistant strains 00-192-RA and 00-192-RB to 4 µg/ml stichloroside and 1 µg/ml theopaluamide.

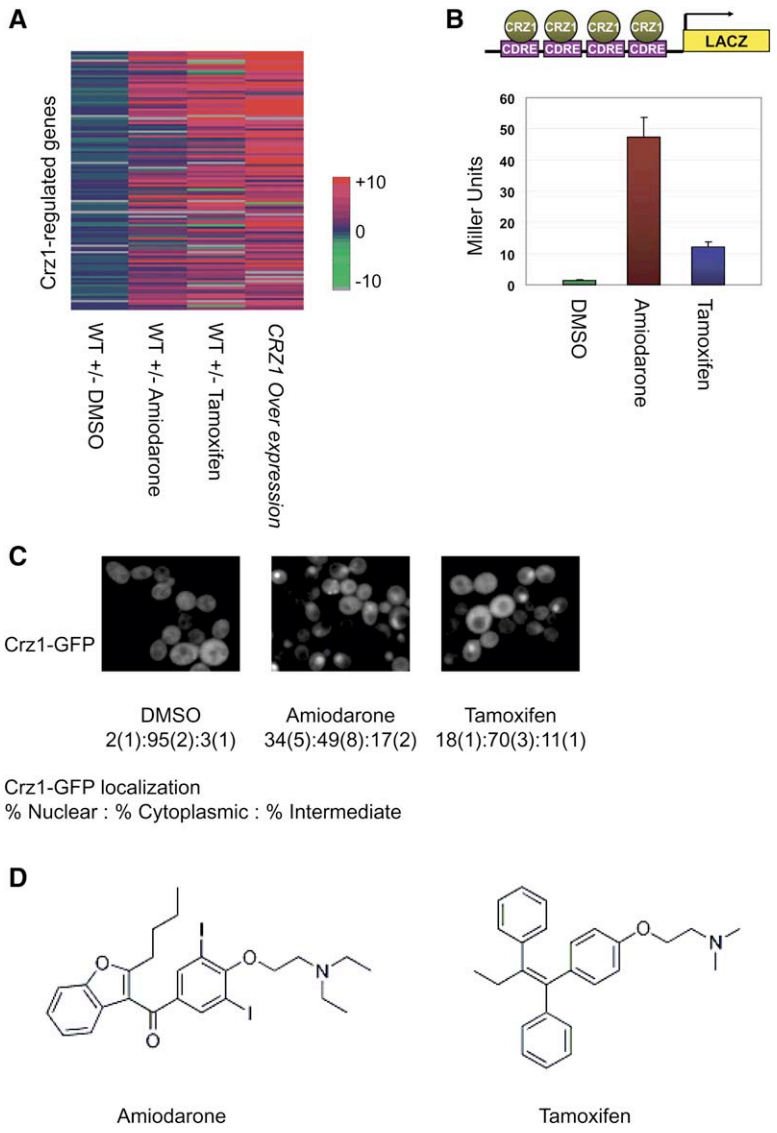

Figure 4. Activation of the Calcineurin/Crz1-Signaling Pathway by Amiodarone and Tamoxifen

(A) Microarray profiling shows the induction of Crz1-regulated gene expression upon drug exposure and overproduction of Crz1. The Crz1-regulated gene list is from Yoshimoto et al. (Yoshimoto et al., 2002). The *CRZ1* overexpression strain (*CRZ1OE*) that contains a Crz1-GST fusion under control of the *GAL1-10* promoter was induced for 3 hr with 2% galactose.

(B) A LacZ reporter driven by the calcineurin-dependent response element (CDRE) is activated by drug treatment.

(C) GFP-Crz1 is translocated into the nucleus within 10 min of drug exposure in amiodarone- and tamoxifen-treated cells. Approximately 1000 cells were counted for nuclear (N), cytoplasic (C), or intermediate (I) localization of GFP-Crz1. Values are the average of three replicate experiments and reported as %N:%C:%I where the error (in parentheses) is the largest difference from the average over the three experiments.

(D) Chemical structures of amiodarone and tamoxifen.

yeast cells may be similar, suggesting that tamoxifen may also produce an increase in cytosolic Ca^{2+} in yeast. To test this possibility, we assayed for the activation of the Ca^{2+}/calcineurin/Crz1 signaling pathway in both drug treatments. In response to high concentrations of external Ca^{2+}, calcineurin induces the transcription of genes required for the cell's adaptation to calcium stress by promoting the nuclear translocation of the transcription factor Crz1. Crz1 subsequently binds to the calcineurin-dependent response element (CDRE) within the promoter regions of the stress-response genes (Matheos et al., 1997; Stathopoulos and Cyert, 1997; Stathopoulos-Gerontides et al., 1999; Yoshimoto et al., 2002). Indeed, both tamoxifen and amiodarone treatments activate the Ca^{2+}/calcineurin/Crz1 signaling pathway, as shown in three independent assays: (1) microarray profiling reveals the induction of Crz1-regulated gene expression upon drug exposure; (2) a LacZ reporter driven by the calcineurin-dependent response element (CDRE) is activated by drug treatment; (3) Crz1 is translocated into the nucleus within 10 min after drug exposure (Figures 4A–4C). The CDRE-lacZ reporter is activated to a greater extent by amiodarone as compared to tamoxifen (Figure 4B) and similarly, amiodarone treatment leads to greater nuclear localization of GFP-Crz1 than tamoxifen (Figure 4C), suggesting that amiodarone is a more potent activator of calcineurin signaling. We also note that, as assessed by GFP-Crz1 localization, tamoxifen appears to be a more potent activator of calcineurin signaling than amantadine and other compounds that cluster near amiodarone and tamoxifen in Figure 1 (Figure S2). Strikingly, tamoxifen and amiodarone share structural similarities (Figure 4D). Thus, our analysis suggests that tamoxifen and amiodarone may be affecting similar pathways in yeast, implying that some of their biological effects may be due to overlapping cellular targets in humans as well. Indeed, there is

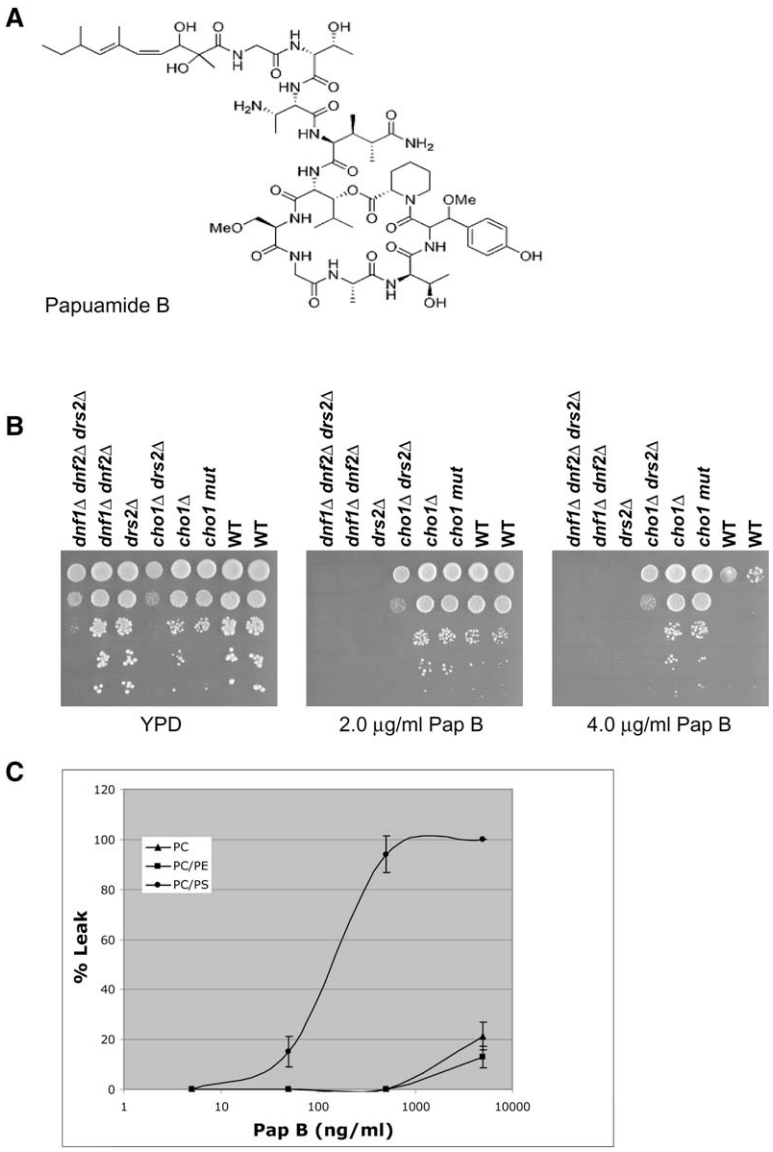

Figure 5. Papuamide B

(A) Cyclic lipopeptide structure of pap B.

(B) Spot dilution assays depicting sensitivity and resistance of various mutants to pap B. *cho1Δ* strains cannot synthesize phosphatidylserine (PS) and strains lacking *DNF1*, *DNF2*, and/or *DRS2* are defective for flipping PS from the outer bilayer of the cell membrane to the inner bilayer, resulting in an excess of PS in the outer membrane. *cho1Δ* and *cho1Δdrs2Δ* strains are resistant to 4 μg/ml pap B whereas *drs2Δ*, *dnf1Δdnf2Δ*, and *dnf1Δdnf2Δdrs2Δ* strains are hypersensitive to 2 μg/ml pap B.

(C) Pap B permeabilizes liposomes containing PS. Release of calcein, a fluorescent marker from 100% PC, 90% PC/10% PE, and 90% PC/10% PS liposomes over a series of pauamide B concentrations was quantified compared to 100% release from liposomes exposed to Triton-X 100. Pap B is approximately 100-fold more potent against PC liposomes with 10% PS than PC liposomes or PC liposomes with 10% PE. Data correspond to the mean values of at least four experiments. Error bars correspond to the standard deviation.

evidence that tamoxifen causes an increase in intracellular free Ca^{2+} concentrations in a number of cell types including renal tubular cells (Jan et al., 2000), breast cells (Chang et al., 2001, 2002), bladder cells (Chang et al., 2001), and Chinese hamster ovary cells (Jan et al., 2003). These non-estrogen receptor-mediated effects cause cytotoxicity at tamoxifen concentrations that are higher than those normally used in the clinic (10^{-6}M) (Jain and Trump, 1997).

Linking Papuamide B to Its Cellular Target, Phosphatidylserine

Papuamide B (pap B), a high-molecular-weight cyclic-lipopeptide originally isolated from a marine sponge, is a cytotoxic compound with anti-HIV activity (Figure 5A) (Ford et al., 1999). Pap B also has potent antifungal activity with an MIC (minimal inhibitory concentration) against *S. cerevisiae* of less than 1 μg/ml (data not shown). The chemical-genetic profile of pap B includes over 300 genes with a $\log_2$ ratio of greater than 1.58, representing a 3-fold or greater underrepresentation of the corresponding deletion strain in the drug treated versus non-drug-treated pool. To identify the top strains that were specifically hypersensitive to individual compounds, we assigned a p value to each chemical-genetic interaction based on a modified Student's t test. This method better highlights chemical-genetic interactions specific to the compound and puts less emphasis on more promiscuous interactions (Lum et al., 2004). The top 50 pap B hits sorted by p value are listed in Table S3 (assigned p values for our complete data set are listed in Table S4). The pap B list is enriched for genes with certain Gene Ontology annotations including vesicle-mediated transport (p = 0.0002958), cell-wall

organization and biogenesis (p = 1.115e-10), and protein modification (p = 0.0003363), suggesting that this compound may affect intracellular transport or perturb some target on the cell surface (Robinson et al., 2002). In addition, we compared the pap B chemical-genetic screen to a set of 132 genome-wide genetic interaction screens (Tong et al., 2004) by hierarchical clustering and found that the pap B screen clustered with genetic screens of cell-surface mutants (Figure S3).

Molecular analysis of several different vesicular trafficking pathways failed to reveal a pap B-specific effect (Figure S4). Because the most recent antifungal drug, caspofungin (Kartsonis et al., 2003), is also a cyclic lipopeptide and it is known to target the yeast cell wall (1-3) β-glucan synthase (Douglas et al., 1994a, 1994b), we tested if pap B perturbed (1-3) β-glucan synthase activity in vitro; however, we observed no effect of pap B in this assay (Figure S5), suggesting that it interacts with a novel cell-surface target.

Because specific drug targets can often be identified through the analysis of drug-resistant mutants (Douglas et al., 1994a, 1994b; Fried and Warner, 1982; Heitman et al., 1991), we isolated pap B-resistant mutants by spotting wild-type cells on rich medium containing high concentrations of pap B. Genetic analysis confirmed that the resistance was associated with a single complementation group and identified a single gene. In addition, we found that the resistant mutant was unable to grow on minimal medium, which enabled us to clone the gene associated with resistance by using a plasmid-based genomic library to complement the minimal medium growth defect. We cloned the *CHO1* gene and, through sequence and subsequent genetic analysis, identified the drug-resistant strain as a *cho1* null mutant.

CHO1 encodes a nonessential enzyme required for the synthesis of PS (Kiyono et al., 1987), one of four major phospholipids that comprise *S. cerevisiae* cell membranes. In the eukaryotic plasma membrane, sphingolipids and phosphotidylcholine (PC) are mainly located in the outer leaflet of the plasma membrane whereas PS and phosphatidylethanolamine (PE) are mainly located in the inner leaflet. This asymmetry is established by aminophospholipid translocases that "flip" PS and PE from the outer leaflet to the inner leaflet. Potential aminophospholipid translocases in yeast include Drs2, Dnf1, and Dnf2 (Natarajan et al., 2004; Pomorski et al., 2003); consequently, *drs2Δ*, *dnf1Δ*, and *dnf2Δ* expose more PS on the outer leaflet of the cell membrane than wild-type cells. If pap B interacts with PS and if this interaction is important for its antifungal activity, then mutants defective for aminophospholipid translocases should be hypersensitive to pap B. Indeed, we found that *drs2Δ*, *dnf1Δdnf2Δ*, and *drs2Δdnf1Δdnf2Δ* cells were hypersensitive to pap B, in contrast to the *cho1Δ* cells which are resistant to pap B (Figure 5B). In addition, ten deletion strains with high $\log_2$ ratios in the pap B screen were assayed for annexin V binding, a PS-specific protein (van Engeland et al., 1998). These mutants bound more annexin V than wild-type cells (Figure S6), suggesting that like *drs2Δ*, these mutants have excess PS on the outer leaflet of their cell membrane, which results in their sensitivity to pap B.

The potential interaction of pap B with PS suggests that the antifungal activity of pap B may result from its ability to bind PS on the plasma membrane and thereby disrupt membrane integrity, leading to inappropriate permeability. To examine this possibility using chemical-genetic profiling, we analyzed a general antimicrobial pore-forming peptide, alamethicin (Bechinger, 1997). If pap B disrupts membrane permeability, then alamethicin and pap B should show similar chemical-genetic profiles. Indeed, we found that pap B and alamethicin cluster together within the compendium (Figure 1, cluster xi) and were also associated together using PMSF analysis (factor profile 5, Figure 2A). Moreover, we also found that the chemical-genetic profile of Ro 09-0198, a peptide that binds PE, inducing transbilayer lipid movement and compromising cell membrane integrity (Makino et al., 2003), also clusters with pap B and alamethicin (Figure S7).

To further test the hypothesis, we studied the effect of pap B on marker release from liposomes containing PS. Strikingly, pap B is about 100-fold more potent against PC liposomes with 10% PS than PC liposomes with 10% PE. Pure PC liposomes were only slightly permeabilized at the highest concentration of pap B tested (Figure 5C). Taken together, these lines of evidence support a mechanism of action for pap B in which it compromises yeast cell membrane integrity through a direct interaction with PS. Interestingly, there is evidence that PS in the outer leaflet of the HIV-1 membrane is required for HIV infection (Callahan et al., 2003), and the PS-specific protein annexin V specifically inhibits HIV infection presumably through its interaction with PS (Callahan et al., 2003), suggesting a similar mechanism for the anti-HIV activity of pap B.

DISCUSSION

Here, we tested the set of yeast viable deletion mutants for hypersensitivity to growth-inhibitory compounds and generated a compendium of chemical-genetic profiles derived from compounds targeted to a number of distinct cellular pathways and functions, including the actin cytoskeleton, the cell wall and cell membrane, ergosterol biosynthesis, the microtubule cytoskeleton, hsp90 chaperone function, protein synthesis and translation, and DNA metabolism. Hierarchical clustering analysis and probabilistic sparse matrix factorization identified similarities between chemical-genetic profiles that often reflect a common biological target or mode-of-action. Thus, this compendium should provide a valuable key for interpreting the cellular effects of novel compounds with similar activities. The continued expansion of the compendium will generate a more sophisticated resource for highly detailed functional classification of compounds, grouping compounds that perturb similar sets of gene deletion mutants,

and genes, identifying sets of deletion mutants that show sensitivity to similar sets of compounds.

Barcode-based chemical-genetic profiling in yeast is relatively simple and robust and is broadly applicable to any compound with growth-inhibitory antifungal activity. We have shown that it works well with both crude natural product extracts as well as purified compounds. A compendium approach to chemical-genetic profiling expands upon the use of haploinsufficiency profiling (HIP) to define compound mode-of-action. In contrast to chemical-genetic profiling of haploid deletion mutants, which often identifies tens to hundreds of deletion mutant hypersensitive strains, the HIP assay generally identifies a relatively small number of potential target genes, often fewer than 10, whose decreased dosage leads to compound hypersensitivity (Baetz et al., 2004; Giaever et al., 1999, 2004; Lum et al., 2004). Thus, while the HIP assay has the potential to identify the target gene, there is less functional information associated with the mutant hypersensitivity signature and thus the two approaches are complementary. Applying chemical-genetic profiling in concert with drug-resistant mutant analysis, we were able to establish a cell-surface phospholipid target for a previously uncharacterized antifungal compound, papuamide B, whereas similar conclusions could not be drawn from the HIP assay mutant hypersensitivity signature (data not shown).

Because a deletion mutant provides a model for the effect of a compound that inhibits the gene product (Marton et al., 1998), genetic interaction information obtained from genome-wide synthetic lethal screens of haploid deletion mutants provides a key for interpreting chemical-genetic profiles and thereby links compounds to their target pathways based on chemical-genetic interaction data alone (Parsons et al., 2004). Chemical-genetic profiling is highly sensitive partly because of the quantitative nature of fitness tests associated with a barcode readout. Synthetic lethal genetic analysis can also be scored with a quantitative assessment of double mutant phenotypes, either through computational analysis of array images (Schuldiner et al., 2005; Tong et al., 2004) or through a barcode microarray readout (Pan et al., 2004). Currently, we have only cataloged 2%–4% of all genetic interactions (Tong et al., 2001, 2004) and so our ability to integrate chemical-genetic and genetic interaction data is limited; however, large-scale application of genetic interaction screening should ultimately provide a detailed key for interpretation of chemical-genetic profiles, such as those described here.

EXPERIMENTAL PROCEDURES

Chemical-Genetic Profiling

Compounds were purchased from Sigma, except for mitomycin C, radicicol, FK506, cytochalasin, brefeldin A, and camptothecin, which were purchased from AG Scientific; Hoechst 3358, which was purchased from Molecular Probes; fenpropimorph, which was purchased from Reidel; and U73122, which was purchased from Calbiochem. Fluconazole was a gift from J. Anderson, geldanamycin was a gift from W. Houry, and caspofungin was a gift from G. Giaever. Natural product extracts, pap B, agelasine E, and basiliskamide A were from the collection of R. Andersen. Compounds were dissolved in DMSO except as noted: trifluoroperaine, pentamidine, nystatin, MMS, mitomycin C, hygromycin B, hydroxyurea, hydroxyethilhidrazine, hydrogen peroxide, fluconazole, emetine, doxycycline, caffeine, anisomycin, actinomycin, thialysin, sodium azide, and clomiphene were dissolved in water; phenantroline, brefeldin A, and artemisinin were dissolved in ethanol; wortmannin was dissolved in methanol; cisplatin was dissolved in a 0.9% sodium chloride solution. Crude extracts were dissolved in methanol.

Chemical-genetic profiling was performed as described (Zhao et al., 2005). For details see Supplemental Experimental Procedures.

Data Preprocessing

For information on data preprocessing, see Supplemental Experimental Procedures.

Clustering Analysis

In each experiment, $\log_2$ ratios of the control divided by sample intensities were computed for each tag. $\log_2$ ratio measurements of up and down tags were averaged, when both were available. In the case where there was only one tag, its value was averaged with the most probable value for a $\log_2$ ratio measurement (approximately zero), effectively weighing down the impact a measurement from a single tag may contribute to the analysis, when the other tag is missing. Two-dimensional hierarchical agglomerative clustering using Pearson's correlation and average linkage was applied to the data using Matlab 7 (The MathWorks). $\log_2$ ratios below 0.5 were set to 0, and only those strains with at least one measurement above 0.5 are shown in the clustogram. Multidrug-sensitive strains were removed from the analysis (see below). For the original data set used to generate the cluster see Table S7 and for the complete clustered data set see Table S8.

Identification of Multidrug-Sensitive Strains

The probability of observing by chance for any given strain as many $\log_2$ ratio measurements above 1.8 as were actually observed was estimated using a hypergeometric distribution (Supplemental Experimental Procedures). A set of commonly resistant strains were also identified (Table S9). Many of these strains have been previously identified as slowly growing diploid homozygous deletion mutant strains (Deutschbauer et al., 2005). In our experiments, we run the control and drug-treated experiments for the same amount of time, such that the control pool undergoes more population doublings than the drug-treated (growth-inhibited) pool. As a result, slowly growing strains may appear relatively enriched, and therefore resistant, in the drug-treated pool compared to the control.

Analysis of Individual Strain Sensitivity

To assess the significance of the effect of a drug on a deletion strain, a t test score and a corresponding p value were calculated based on the $\log_2$ ratio measurements of growth of that strain in the presence of that particular drug, with respect to all other measurements obtained for that strain under all 82 conditions (Lum et al., 2004). For calculation details see Supplemental Experimental Procedures.

PSMF Analysis

The data were analyzed using probabilistic sparse matrix factorization (Dueck et al., 2005; Software available at http://www.psi.toronto.ca/factorgram) applied to a data matrix X of 4111 deletion mutant strains by 82 compounds, containing all chemical-genetic interactions after removal of nonfunctional tags, multidrug-sensitive strains, and strains that do not appear in ORF gene ontology list from SGD (Table S6). Negative scores were set to 0. For further details regarding this analysis, see Supplemental Experimental Procedures. The figure was produced using a factorgram visualization tool (Cheung et al., 2006), available at the above website.

Microarray Profiling

Untreated wild-type cells BY4743 (all strain genotypes are listed in the Supplemental Experimental Procedures) were logarithmically grown in parallel with cultures treated with DMSO (0.2%), tamoxifen (20 μg/ml), and amiodarone (200 μg/ml) for 1.5 hr. For the overexpression of *CRZ1*, strains containing a 2μ-based plasmid encoding a Crz1-GST fusion driven by the *GAL1-10* promoter or an empty vector control (pEGH) were grown concurrently in selective media supplemented with 2% raffinose to mid-log phase followed by induction in 2% galactose for 3 hr. Cells were harvested by centrifugation (3000 RPM, 2 min) and immediately frozen in liquid nitrogen. RNA preparation, hybridization, image acquisition, and processing of microarrays were performed as described (Grigull et al., 2004).

β-Galactosidase Assays

The strain ASY822 (Kafadar et al., 2003), which contains a *LacZ* reporter driven by four tandem copies of the calcineurin-dependent response element (CDRE), was treated with 0.2% DMSO, 10 μg/ml tamoxifen, and 50 μg/ml amiodarone for 1.5 hr, and β-galactosidase activity was measured (Rose and Botstein, 1983).

CRZ1 Translocation Assay

An overnight culture (Y2454 + pMET-3xGFP-Crz1 [pLMB127]) in SD-URA was diluted in SD-URA MET and grown to mid-log phase (about 5 hr). Cells were harvested and resuspended in YPD. Drug was added to a final concentration of 10 μg/ml for tamoxifen, 50 μg/ml for amidarone, 19 μg/ml for amantadine hydrochloride, and 15 μg/ml clomiphene. One milliliter samples were spun down and examined after 10 min. Cells were visualized by epifluorescence microscopy with a GFP filter and a 1000 ms exposure time.

Natural Product Extracts and Compound Derivation

Crude natural products were dissolved in methanol for a final stock concentration of 10 mg/ml. Compounds were derived from natural product extracts using methanol extraction as described (Williams et al., 2005).

Growth Curves

From overnight YPD cultures, yeast strains Y1239, Y6883, and Y6882 were diluted to an OD600 of 0.05 in 3 ml cultures. Stichloroside (4 μg/ml), theopaluamide (1 μg/ml), or 1% DMSO were added to the cultures. Cultures were incubated at 30°C while shaking and ODs were recorded every 90 min. Seven time points were taken. Each growth curve was tested at least twice and representative curves are shown.

Generation of Resistant Mutants

Wild-type yeast BY4741a was spotted (3 μl spots of OD 1 culture) onto YPD agar plates containing inhibitory concentrations of drug (4 μg/ml pap B or 50 μg/ml extract 00-192). Plates were incubated for 3 to 4 days to allow resistant mutants to grow up. Resistant colonies were confirmed by restreaking single colonies onto drug-containing media. Seven pap B-resistant mutants were identified. Standard tetrad analysis confirmed that resistance in each strain was conferred by a recessive mutation in a single gene. Six of the seven mutants were classified into one complementation group (Pap B-R1), which was later confirmed as a *CHO1* mutant (see below). The remaining pap B-resistant mutant remains unidentified. Four mutants were confirmed as resistant to extract 00-192. Resistance was a recessive trait resulting from mutation of a single gene in each case. Three mutants were classified as belonging to complementation group 1 (00-192-RA) and the fourth to complementation group 2 (00-192-RB).

Cloning of Pap B-Resistant Mutant

The pap B-resistant strain Y6531 was transformed with a high-copy (Yep24) yeast genomic library. Transformants were selected on SD-URA then replica-plated onto minimal media (*PapB-R1* confers a growth defect on minimal media). Plasmids were extracted from those transformants that grew on minimal media and inserts were sequenced, revealing that all plasmids contained the *CHO1* gene.

Pap B Spot Assays

Yeast strains Y1239, Y7688, Y7689, Y7690, Y7691, and Y6531 were grown overnight in YPD. Cultures were diluted in YPD to OD1. Two microliter spots of 10× dilutions were spotted onto YPD agar plates containing no drug, 2 μg/ml pap B, and 4 μg/ml pap B. Plates were incubated for 2 days at 30°C and photographed.

Liposome Assay

Large unilamellar vesicles (LUVs) were prepared by filter extrusion in the presence of 5 mM calcein, a fluorescent compound that self-quenches at high concentrations. LUVs were prepared from 100% PC (PC), 90% PC/10% PE (PC/PE), or 90% PC/10%PS (PC/PS) and dialyzed overnight to remove external, untrapped calcein. Leakage of calcein from the liposomes was measured by increase in fluorescence (reduction of quenching upon dilution) at room temperature in 2 ml of TNE (10 mM Tris-Cl pH 7.4, 154 mM NaCl, and 0.1 mM EDTA) containing ~50 μg LUVs. Baseline fluorescence of LUVs was determined before Pap B addition and 100% leakage determined by addition of Triton X-100 to 0.1% after Pap B addition.

Supplemental Data

Supplemental Data include experimental procedures, seven figures, and nine tables and can be found with this article online at http://www.cell.com/cgi/content/full/126/3/611/DC1/.

ACKNOWLEDGMENTS

We thank J. Anderson, G. Giaever, and W. Houry for gifts of fluconazole, caspofungin, and geldanamycin, respectively. We thank M. Umeda for the Ro peptide and we thank M. Cyert for the CDRE-lacZ reporter. This work was supported by grants from the Canadian Institute of Health Research (CIHR) to C.B., R.J.A., and T.R.H.; NIH GM72119 to G.E.F.; and NIH GM67911 to G.S.P. A.B.P. holds a CIHR graduate student fellowship.

Received: January 15, 2006
Revised: March 31, 2006
Accepted: June 6, 2006
Published: August 10, 2006

REFERENCES

Aoun, M. (2000). Standard antifungal therapy in neutropenic patients. Int. J. Antimicrob. Agents *16*, 143–145.

Ayscough, K.R., Stryker, J., Pokala, N., Sanders, M., Crews, P., and Drubin, D.G. (1997). High rates of actin filament turnover in budding yeast and roles for actin in establishment and maintenance of cell polarity revealed using the actin inhibitor latrunculin-A. J. Cell Biol. *137*, 399–416.

Baetz, K., McHardy, L., Gable, K., Tarling, T., Reberioux, D., Bryan, J., Andersen, R.J., Dunn, T., Hieter, P., and Roberge, M. (2004). Yeast genome-wide drug-induced haploinsufficiency screen to determine drug mode of action. Proc. Natl. Acad. Sci. USA *101*, 4525–4530.

Bechinger, B. (1997). Structure and functions of channel-forming peptides: magainins, cecropins, melittin and alamethicin. J. Membr. Biol. *156*, 197–211.

Brown, J.A., Sherlock, G., Myers, C.L., Burrows, N.M., Deng, C., Wu, H.I., McCann, K.E., Troyanskaya, O.G., and Brown, J.M. (2006). Global analysis of gene function in yeast by quantitative phenotypic profiling. Mol. Syst. Biol. *2*, 0001.

Callahan, M.K., Popernack, P.M., Tsutsui, S., Truong, L., Schlegel, R.A., and Henderson, A.J. (2003). Phosphatidylserine on HIV envelope

is a cofactor for infection of monocytic cells. J. Immunol. *170*, 4840–4845.

Chang, H.T., Huang, J.K., Wang, J.L., Cheng, J.S., Lee, K.C., Lo, Y.K., Lin, M.C., Tang, K.Y., and Jan, C.R. (2001). Tamoxifen-induced Ca2+ mobilization in bladder female transitional carcinoma cells. Arch. Toxicol. *75*, 184–188.

Chang, H.T., Huang, J.K., Wang, J.L., Cheng, J.S., Lee, K.C., Lo, Y.K., Liu, C.P., Chou, K.J., Chen, W.C., Su, W., et al. (2002). Tamoxifen-induced increases in cytoplasmic free Ca2+ levels in human breast cancer cells. Breast Cancer Res. Treat. *71*, 125–131.

Cheng, Y., and Church, G.M. (2000). Biclustering of expression data. Proc. Int. Conf. Intell. Syst. Mol. Biol. *8*, 93–103.

Cheung, V., Givoni, I., Dueck, D., and Frey, B.J. (2006). Factorgrams: A tool for visualizing multi-way associations in biological data (University of Toronto Technical Report PSI-2006-44) *May 15*, 2006.

Courchesne, W.E. (2002). Characterization of a novel, broad-based fungicidal activity for the antiarrhythmic drug amiodarone. J. Pharmacol. Exp. Ther. *300*, 195–199.

Courchesne, W.E., and Ozturk, S. (2003). Amiodarone induces a caffeine-inhibited, MID1-depedent rise in free cytoplasmic calcium in Saccharomyces cerevisiae. Mol. Microbiol. *47*, 223–234.

Deutschbauer, A.M., Jaramillo, D.F., Proctor, M., Kumm, J., Hillenmeyer, M.E., Davis, R.W., Nislow, C., and Giaever, G. (2005). Mechanisms of haploinsufficiency revealed by genome-wide profiling in yeast. Genetics *169*, 1915–1925.

Douglas, C.M., Foor, F., Marrinan, J.A., Morin, N., Nielsen, J.B., Dahl, A.M., Mazur, P., Baginsky, W., Li, W., el-Sherbeini, M., et al. (1994a). The Saccharomyces cerevisiae FKS1 (ETG1) gene encodes an integral membrane protein which is a subunit of 1,3-beta-D-glucan synthase. Proc. Natl. Acad. Sci. USA *91*, 12907–12911.

Douglas, C.M., Marrinan, J.A., Li, W., and Kurtz, M.B. (1994b). A Saccharomyces cerevisiae mutant with echinocandin-resistant 1,3-beta-D-glucan synthase. J. Bacteriol. *176*, 5686–5696.

Dueck, D., Morris, Q.D., and Frey, B.J. (2005). Multi-way clustering of microarray data using probabilistic sparse matrix factorization. Bioinformatics *21* (Suppl 1), i144–i151.

Flaherty, P., Giaever, G., Kumm, J., Jordan, M.I., and Arkin, A.P. (2005). A latent variable model for chemogenomic profiling. Bioinformatics *21*, 3286–3293.

Ford, P.W., Gustafson, K.R., McKee, T., Shigematsu, N., Maurizi, L., Pannell, L., Williams, D., Dilip de Silva, E., Lassota, P., Allen, T., et al. (1999). Papuamides A-D, HIV-inhibitory and cytotoxic depsipeptides from the sponges theonella mirabilis and theonella swinhoei collected in Papua New Guinea. J. Am. Chem. Soc. *121*, 5899–5909.

Fried, H.M., and Warner, J.R. (1982). Molecular cloning and analysis of yeast gene for cycloheximide resistance and ribosomal protein L29. Nucleic Acids Res. *10*, 3133–3148.

Fromtling, R.A. (1988). Overview of medically important antifungal azole derivatives. Clin. Microbiol. Rev. *1*, 187–217.

Giaever, G., Shoemaker, D.D., Jones, T.W., Liang, H., Winzeler, E.A., Astromoff, A., and Davis, R.W. (1999). Genomic profiling of drug sensitivities via induced haploinsufficiency. Nat. Genet. *21*, 278–283.

Giaever, G., Chu, A.M., Ni, L., Connelly, C., Riles, L., Veronneau, S., Dow, S., Lucau-Danila, A., Anderson, K., Andre, B., et al. (2002). Functional profiling of the Saccharomyces cerevisiae genome. Nature *418*, 387–391.

Giaever, G., Flaherty, P., Kumm, J., Proctor, M., Nislow, C., Jaramillo, D.F., Chu, A.M., Jordan, M.I., Arkin, A.P., and Davis, R.W. (2004). Chemogenomic profiling: identifying the functional interactions of small molecules in yeast. Proc. Natl. Acad. Sci. USA *101*, 793–798.

Grigull, J., Mnaimneh, S., Pootoolal, J., Robinson, M.D., and Hughes, T.R. (2004). Genome-wide analysis of mRNA stability using transcription inhibitors and microarrays reveals posttranscriptional control of ribosome biogenesis factors. Mol. Cell. Biol. *24*, 5534–5547.

Gupta, S.S., Ton, V.K., Beaudry, V., Rulli, S., Cunningham, K., and Rao, R. (2003). Antifungal activity of amiodarone is mediated by disruption of calcium homeostasis. J. Biol. Chem. *278*, 28831–28839.

Heitman, J., Movva, N.R., and Hall, M.N. (1991). Targets for cell cycle arrest by the immunosuppressant rapamycin in yeast. Science *253*, 905–909.

Hernandez, F., and Cannon, M. (1982). Inhibition of protein synthesis in Saccharomyces cerevisiae by the 12,13-epoxytrichothecenes trichodermol, diacetoxyscirpenol and verrucarin A. Reversibility of the effects. J. Antibiot. (Tokyo) *35*, 875–881.

Hosono, K. (2000). Effect of nystatin on the release of glycerol from salt-stressed cells of the salt-tolerant yeast Zygosaccharomyces rouxii. Arch. Microbiol. *173*, 284–287.

Hughes, T.R., Marton, M.J., Jones, A.R., Roberts, C.J., Stoughton, R., Armour, C.D., Bennett, H.A., Coffey, E., Dai, H., He, Y.D., et al. (2000). Functional discovery via a compendium of expression profiles. Cell *102*, 109–126.

Jain, P.T., and Trump, B.F. (1997). Tamoxifen induces deregulation of [Ca2+] in human breast cancer cells. Anticancer Res. *17*, 1167–1174.

Jan, C.R., Cheng, J.S., Chou, K.J., Wang, S.P., Lee, K.C., Tang, K.Y., Tseng, L.L., and Chiang, H.T. (2000). Dual effect of tamoxifen, an anti-breast-cancer drug, on intracellular Ca(2+) and cytotoxicity in intact cells. Toxicol. Appl. Pharmacol. *168*, 58–63.

Jan, C.R., An-Jen, C., Chang, H.T., Roan, C.J., Lu, Y.C., Jiann, B.P., Ho, C.M., and Huang, J.K. (2003). The anti-breast cancer drug tamoxifen alters Ca2+ movement in Chinese hamster ovary (CHO-K1) cells. Arch. Toxicol. *77*, 160–166.

Kafadar, K.A., Zhu, H., Snyder, M., and Cyert, M.S. (2003). Negative regulation of calcineurin signaling by Hrr25p, a yeast homolog of casein kinase I. Genes Dev. *17*, 2698–2708.

Kartsonis, N.A., Nielsen, J., and Douglas, C.M. (2003). Caspofungin: the first in a new class of antifungal agents. Drug Resist. Updat. *6*, 197–218.

Kitagawa, I., Kobayashi, M., Imamoto, T., Yasuzawa, T., and Kyogoku, Y. (1981). The structures of six antifungal oligoglycosides, stichlorosides A1, A2, B1, B2, C1 and C2, from the sea cucumber Stichopus chloronotus (BRANDT). Chem. Pharm. Bull. (Tokyo) *29*, 2387–2391.

Kiyono, K., Miura, K., Kushima, Y., Hikiji, T., Fukushima, M., Shibuya, I., and Ohta, A. (1987). Primary structure and product characterization of the Saccharomyces cerevisiae CHO1 gene that encodes phosphatidylserine synthase. J. Biochem. (Tokyo) *102*, 1089–1100.

Kunkel, W. (1980). Effects of the antimicrotubular cancerostatic drug nocodazole on the yeast Saccharomyces cerevisiae. Z. Allg. Mikrobiol. *20*, 315–324.

Lee, W., St Onge, R.P., Proctor, M., Flaherty, P., Jordan, M.I., Arkin, A.P., Davis, R.W., Nislow, C., and Giaever, G. (2005). Genome-wide requirements for resistance to functionally distinct DNA-damaging agents. PLoS Genet *1*, e24. 10.1371/journal.pgen.0010024.

Lum, P.Y., Armour, C.D., Stepaniants, S.B., Cavet, G., Wolf, M.K., Butler, J.S., Hinshaw, J.C., Garnier, P., Prestwich, G.D., Leonardson, A., et al. (2004). Discovering modes of action for therapeutic compounds using a genome-wide screen of yeast heterozygotes. Cell *116*, 121–137.

Makino, A., Baba, T., Fujimoto, K., Iwamoto, K., Yano, Y., Terada, N., Ohno, S., Sato, S.B., Ohta, A., Umeda, M., et al. (2003). Cinnamycin (Ro 09–0198) promotes cell binding and toxicity by inducing transbilayer lipid movement. J. Biol. Chem. *278*, 3204–3209.

Marcireau, C., Guilloton, M., and Karst, F. (1990). In vivo effects of fenpropimorph on the yeast Saccharomyces cerevisiae and determination of the molecular basis of the antifungal property. Antimicrob. Agents Chemother. *34*, 989–993.

Marton, M.J., DeRisi, J.L., Bennett, H.A., Iyer, V.R., Meyer, M.R., Roberts, C.J., Stoughton, R., Burchard, J., Slade, D., Dai, H., et al. (1998). Drug target validation and identification of secondary drug target effects using DNA microarrays. Nat. Med. *4*, 1293–1301.

Matheos, D.P., Kingsbury, T.J., Ahsan, U.S., and Cunningham, K.W. (1997). Tcn1p/Crz1p, a calcineurin-dependent transcription factor that differentially regulates gene expression in Saccharomyces cerevisiae. Genes Dev. *11*, 3445–3458.

Moebius, F.F., Bermoser, K., Reiter, R.J., Hanner, M., and Glossmann, H. (1996). Yeast sterol C8–C7 isomerase: identification and characterization of a high-affinity binding site for enzyme inhibitors. Biochemistry *35*, 16871–16878.

Natarajan, P., Wang, J., Hua, Z., and Graham, T.R. (2004). Drs2p-coupled aminophospholipid translocase activity in yeast Golgi membranes and relationship to in vivo function. Proc. Natl. Acad. Sci. USA *101*, 10614–10619.

Pan, X., Yuan, D.S., Xiang, D., Wang, X., Sookhai-Mahadeo, S., Bader, J.S., Hieter, P., Spencer, F., and Boeke, J.D. (2004). A robust toolkit for functional profiling of the yeast genome. Mol. Cell *16*, 487–496.

Parsons, A.B., Brost, R.L., Ding, H., Li, Z., Zhang, C., Sheikh, B., Brown, G.W., Kane, P.M., Hughes, T.R., and Boone, C. (2004). Integration of chemical-genetic and genetic interaction data links bioactive compounds to cellular target pathways. Nat. Biotechnol. *22*, 62–69.

Pomorski, T., Lombardi, R., Riezman, H., Devaux, P.F., van Meer, G., and Holthuis, J.C. (2003). Drs2p-related P-type ATPases Dnf1p and Dnf2p are required for phospholipid translocation across the yeast plasma membrane and serve a role in endocytosis. Mol. Biol. Cell *14*, 1240–1254.

Robinson, M.D., Grigull, J., Mohammad, N., and Hughes, T.R. (2002). FunSpec: a web-based cluster interpreter for yeast. BMC Bioinformatics *3*, 35.

Roe, S.M., Prodromou, C., O'Brien, R., Ladbury, J.E., Piper, P.W., and Pearl, L.H. (1999). Structural basis for inhibition of the Hsp90 molecular chaperone by the antitumor antibiotics radicicol and geldanamycin. J. Med. Chem. *42*, 260–266.

Rose, M., and Botstein, D. (1983). Structure and function of the yeast URA3 gene. Differentially regulated expression of hybrid beta-galactosidase from overlapping coding sequences in yeast. J. Mol. Biol. *170*, 883–904.

Schmidt, E.W., Bewley, C.A., and Faulkner, D.J. (1998). Theopalauamide, a bicyclic glycopeptide from filamentous bacterial symbionts of the lithistid sponge Theonella swinhoei from Palau and Mozambique. J. Org. Chem. *63*, 1254–1258.

Schroeder, R., Waldsich, C., and Wank, H. (2000). Modulation of RNA function by aminoglycoside antibiotics. EMBO J. *19*, 1–9.

Schuldiner, M., Collins, S.R., Thompson, N.J., Denic, V., Bhamidipati, A., Punna, T., Ihmels, J., Andrews, B., Boone, C., Greenblatt, J.F., et al. (2005). Exploration of the function and organization of the yeast early secretory pathway through an epistatic miniarray profile. Cell *123*, 507–519.

Shoemaker, D.D., Lashkari, D.A., Morris, D., Mittmann, M., and Davis, R.W. (1996). Quantitative phenotypic analysis of yeast deletion mutants using a highly parallel molecular bar-coding strategy. Nat. Genet. *14*, 450–456.

Sobell, H.M. (1985). Actinomycin and DNA transcription. Proc. Natl. Acad. Sci. USA *82*, 5328–5331.

Stathopoulos, A.M., and Cyert, M.S. (1997). Calcineurin acts through the CRZ1/TCN1-encoded transcription factor to regulate gene expression in yeast. Genes Dev. *11*, 3432–3444.

Stathopoulos-Gerontides, A., Guo, J.J., and Cyert, M.S. (1999). Yeast calcineurin regulates nuclear localization of the Crz1p transcription factor through dephosphorylation. Genes Dev. *13*, 798–803.

Thomas, J.H., Neff, N.F., and Botstein, D. (1985). Isolation and characterization of mutations in the beta-tubulin gene of Saccharomyces cerevisiae. Genetics *111*, 715–734.

Tong, A.H., Evangelista, M., Parsons, A.B., Xu, H., Bader, G.D., Page, N., Robinson, M., Raghibizadeh, S., Hogue, C.W., Bussey, H., et al. (2001). Systematic genetic analysis with ordered arrays of yeast deletion mutants. Science *294*, 2364–2368.

Tong, A.H., Lesage, G., Bader, G.D., Ding, H., Xu, H., Xin, X., Young, J., Berriz, G.F., Brost, R.L., Chang, M., et al. (2004). Global mapping of the yeast genetic interaction network. Science *303*, 808–813.

Torralba, S., Raudaskoski, M., Pedregosa, A.M., and Laborda, F. (1998). Effect of cytochalasin A on apical growth, actin cytoskeleton organization and enzyme secretion in Aspergillus nidulans. Microbiol. *144*, 45–53.

Truan, G., Epinat, J.C., Rougeulle, C., Cullin, C., and Pompon, D. (1994). Cloning and characterization of a yeast cytochrome b5-encoding gene which suppresses ketoconazole hypersensitivity in a NADPH-P-450 reductase-deficient strain. Gene *142*, 123–127.

van Engeland, M., Nieland, L.J., Ramaekers, F.C., Schutte, B., and Reutelingsperger, C.P. (1998). Annexin V-affinity assay: a review on an apoptosis detection system based on phosphatidylserine exposure. Cytometry *31*, 1–9.

Williams, D.E., Patrick, B.O., Behrisch, H.W., Van Soest, R., Roberge, M., and Andersen, R.J. (2005). Dominicin, a cyclic octapeptide, and laughine, a bromopyrrole alkaloid, isolated from the Caribbean marine sponge Eurypon laughlini. J. Nat. Prod. *68*, 327–330.

Yoshida, S., Ikeda, E., Uno, I., and Mitsuzawa, H. (1992). Characterization of a staurosporine- and temperature-sensitive mutant, stt1, of Saccharomyces cerevisiae: STT1 is allelic to PKC1. Mol. Gen. Genet. *231*, 337–344.

Yoshimoto, H., Saltsman, K., Gasch, A.P., Li, H.X., Ogawa, N., Botstein, D., Brown, P.O., and Cyert, M.S. (2002). Genome-wide analysis of gene expression regulated by the calcineurin/Crz1p signaling pathway in Saccharomyces cerevisiae. J. Biol. Chem. *277*, 31079–31088.

Zhao, R., Davey, M., Hsu, Y.C., Kaplanek, P., Tong, A., Parsons, A.B., Krogan, N., Cagney, G., Mai, D., Greenblatt, J., et al. (2005). Navigating the chaperone network: an integrative map of physical and genetic interactions mediated by the hsp90 chaperone. Cell *120*, 715–727.